Journal of
Manufacturing and Materials Processing

MDPI

Article

Multi-Response Optimization of Milling Parameters of AISI D2 Steel Using Response Surface Methodology and Desirability Function

Luis W. Hernández [1,2], Yassmin Seid Ahmed [3,4,*], Dagnier A. Curra [5] and Roberto Pérez [2]

[1] Department of Physics and Engineering, Bindura University of Science Education, Bindura 12100, Zimbabwe; wilfredo.uho@gmail.com
[2] CAD/CAM Study Centre, University of Holguin, Holguin 80100, Cuba; roberto.perez@uho.edu.cu
[3] Mechanical Engineering Department, King Fahd University of Petroleum & Minerals, Dhahran 31261, Saudi Arabia
[4] Interdisciplinary Research Center for Advanced Materials, King Fahd University of Petroleum & Minerals, Dhahran 31261, Saudi Arabia
[5] Departamento de Arquitectura y Tecnología de Computadores, Universidad de Sevilla, 41004 Sevilla, Spain; dcurra85@gmail.com
* Correspondence: yassmin.seidahmed@kfupm.edu.sa

Abstract

This study investigates multi-objective optimization of end-milling parameters for AISI D2 cold-worked tool steel using GC1130-coated carbide inserts under wet machining, focusing on cutting speed and feed rate per tooth values beyond manufacturer recommendations. The objective was to identify parameter settings that minimize surface roughness while maximizing cutting tool life—two performance criteria that often conflict in practice. A full-factorial design of experiments was implemented, varying the cutting speed (220–310 m/min) and feed rate (0.06–0.25 mm/tooth). Response Surface Methodology (RSM) was used to develop predictive models, and a desirability function approach (DFA) was applied to perform multi-response optimization under three weighting schemes. The statistical models showed strong reliability, with R^2 values of 81.09% for surface roughness and 95.02% for tool life. The optimal settings—220 m/min cutting speed and 0.25 mm/tooth feed—resulted in a tool life of 11.03 min and surface roughness of 0.587 µm. This yielded the highest desirability index (D = 0.8706) under tool-life-prioritized weighting, outperforming other cases by up to 10.69%. These findings offer a practical balance between quality and durability, especially for applications where tool wear is a limiting factor.

Keywords: cutting tool life; milling; response surface methodology; desirability function; surface roughness

Academic Editor: Shuting Lei

Received: 4 August 2025
Revised: 7 September 2025
Accepted: 11 September 2025
Published: 13 September 2025

Citation: Hernández, L.W.; Seid Ahmed, Y.; Curra, D.A.; Pérez, R. Multi-Response Optimization of Milling Parameters of AISI D2 Steel Using Response Surface Methodology and Desirability Function. *J. Manuf. Mater. Process.* **2025**, *9*, 314. https://doi.org/10.3390/jmmp9090314

1. Introduction

The production of components through casting or plastic deformation, including moulds and dies, has become increasingly complex. On the one hand, rising quality standards necessitate superior outcomes, while on the other, competitive pressures demand reduced production time and costs.

The pursuit of higher manufacturing quality is relentless. Discerning consumers and strict industry regulations demand products that excel in functionality, aesthetics, and precision. To meet these demands, manufacturers must continually refine mould and die production, achieving ever-greater accuracy.

At the same time, maintaining competitiveness requires constant optimization. Manufacturers must streamline their processes, cutting both time and expenses, as agility and cost-efficiency are key in today's global market.

Ongoing research explores innovative manufacturing methods, with cutting-edge technologies opening up new possibilities. Advanced tools, such as digital modeling and simulation, now enable optimized mould and die design, striking a balance between precision and efficiency.

Fostering strong integration among industries, tool and material suppliers, research centers, and universities is essential. This collaboration is particularly crucial for mould and die manufacturers, who serve as key suppliers to the automotive, agricultural machinery, and other industrial sectors. By working closely together, these manufacturers can reduce costs and enhance their market competitiveness.

The same principle applies to related industries, including forging, general metalworking, plastics production, and component manufacturing. A unified approach ensures efficiency, innovation, and sustainability across the entire supply chain.

Analyzing surface roughness formation in machining enables the accurate prediction of quality, process optimization, cost reduction, and improved sustainability in industrial production [1].

High-speed machining research has also demonstrated significant improvements in finishing performance, process planning, and force characterization for complex parts and advanced steels [2–5]. These works establish a strong foundation for extending process parameters beyond catalog recommendations and motivate further exploration in tool–workpiece performance.

In manufacturing, milling is a fundamental metalworking process, with end-milling being the most common operation used to create profiles, grooves, contours, and cavities. During machining, cutting tools experience gradual material loss, known as tool wear, which significantly affects part quality. Excessive tool wear can impair dimensional accuracy, surface finish, and geometric precision, leading to defective products and higher production costs. Consequently, monitoring and managing tool wear is crucial for maintaining efficiency and product quality [6]. Recent advances in tool wear monitoring—particularly in broaching and electromechanical processes—have highlighted the value of early detection methods for reducing production errors and enhancing reliability [7,8]. While our study employs experimental wear evaluation, such data-driven approaches point to promising directions for future research. Effective collaboration among industry stakeholders, coupled with a comprehensive understanding of tool wear phenomena in metal cutting, is essential for advancing product quality and sustaining competitiveness within the manufacturing sector.

Cutting speed and feed rate are critical parameters that significantly influence surface roughness, tool wear, and productivity. While higher feed rates improve material removal rates, they often compromise surface roughness and accelerate cutting tool wear. Conversely, increasing cutting speed typically enhances surface smoothness but raises cutting temperatures, leading to premature tool degradation. Balancing these parameters is essential to optimize machining performance.

This review highlights significant research on milling processes for cold-worked tool steels. Studies in this field focus on optimizing machining parameters, mitigating tool wear, and maintaining surface integrity, as illustrated in the following sections.

Recent research has extensively analyzed machining parameters—such as cutting speed, feed rate, and tool geometry—and their impact on the hard milling of AISI D3 and D2 tool steels under varying conditions. This review examines foundational studies that

have advanced the understanding of process mechanics, tool wear behavior, and surface integrity in these high-precision machining operations.

Iqbal et al. [9] compared dry and Minimum-Quantity-Lubrication (MQL) machining using TiAlN-coated end-mills. Their research demonstrated that increasing cutting speed and feed rate has detrimental effects on cutting tool life and surface roughness. Furthermore, cutting speed was found to be the most influential parameter affecting these responses. The analyses revealed that MQL significantly enhanced cutting tool life. In a separate study reported in [10], researchers examined the relationships between cutting speed, feed rate, and tool life during high-speed milling of AISI D2 steel using ball-end-mills. The study found that at lower cutting speeds, sintered carbide inserts had significantly higher tool life than cubic boron nitride (CBN) inserts. The study's outcomes offer valuable guidance for optimizing tool life and managing cutting forces in high-speed milling applications. Another noteworthy investigation, detailed in [11], examined cutting forces and vibrations during the milling of AISI D2 steel with ball-nose tools constructed from both coated carbide and cubic boron nitride. The authors found that vibrations generated in a stable milling operation are strongly affected by the tool wear width. This finding deepened the understanding of the tool material's influence on the machining process. Mariño and Sánchez [12] evaluated dry and MQL machining of hardened AISI D2 and D6 steels using constant cutting parameters. Their study found that dry machining yielded longer tool life, whereas MQL machining achieved lower surface roughness values. Research [13] on MoS_2 nanofluid in MQCL-assisted milling examined how nanoparticle concentration, cutting speed, and material hardness affect cutting forces. The findings are useful for optimizing nanoparticle concentration and selecting cutting speeds. Chattopadhyay et al. [14] found that vibration acceleration increased with cutting speed within a specific range, while acoustic pressure increased with both depth of cut and cutting speed. They also reported that increasing cutting speed reduced surface roughness, whereas feed rate and cutting depth had opposing effects (on roughness). However, the correlation between tool wear and surface roughness was not analyzed. Comparing dry and cryogenic hard milling of AISI D3 steel with uncoated tools, Ravi and Gurusamy [15] found that cryogenic cooling improved cutting forces and surface finish. However, flank wear increased at higher cutting speeds, especially in the lower ranges studied. Cryogenic processing consistently outperformed dry machining in all evaluated performance metrics.

Hard milling of AISI D3 and D2 tool steels has been extensively studied to optimize machining performance. This review examines key studies analyzing process mechanics, tool wear, and surface integrity, providing actionable guidelines for industry practitioners.

Evaluating power consumption, feed rates, machine efficiency, and surface roughness in AISI D3 hard milling at conventional speeds, Vila et al. [16] found that surface roughness increased with higher feed rates and cutting speed. This relationship is crucial for guiding the selection of energy-efficient parameters. Saedon et al. [17] investigated dry micromilling of hardened AISI D2 steel, focusing on cutting temperature, microstructure, surface roughness, and microhardness. Their analysis provided key insights into the micromechanics and highlighted specific surface integrity challenges associated with unlubricated micromachining. Gaitonde et al. [18] revealed that cutting temperature increases linearly with cutting speed, while surface roughness increases non-linearly. Additionally, they found that at higher feed rates, increased cutting speed considerably reduces cutting force within a specified depth of cut range. Tlhabadira et al. [19] analyzed the influence of cutting parameters on surface roughness during AISI D2 hard milling using carbide inserts. They found that feed rate was the dominant factor, with higher feed rates having a negative impact on surface roughness. In contrast, increasing the cutting speed improved surface finish, while the depth of cut had a comparatively minor effect. Comparing two MQL

approaches, Mashood et al. [20] found that nanofluid MQL effectively lowered the tool-workpiece interface temperature while enhancing the surface finish. These improvements underscore its suitability for precision machining. Another study by Huang et al. [21] focused on optimizing ball-end hard milling parameters using Response Surface Methodology, prioritizing surface integrity, wear resistance, and fatigue resistance to enhance the durability of precision components. This research has demonstrated that a combination of high spindle speed, small feed per tooth, and small radial depth of cut can meet the requirements for both wear resistance and machining efficiency. Nguyen and Do [22] investigate the intricate relationship between cutting parameters and nanoparticle concentration, as well as their influence on surface roughness and material removal rate during the milling of AISI D2 steel under MQL conditions using SiO_2 nanoparticles. The study showed that the strongest influences on surface roughness are feed rate and nanoparticle concentration, achieving both the minimum surface roughness and the maximum material removal rate. Existing studies on hard milling of AISI D2/D3 steels have overlooked cutting tool wear analysis. Addressing this gap is critical, as tool wear directly impacts machining precision and longevity. Future work should integrate tool wear evaluation to optimize surface finish and tool longevity in demanding applications.

Recent research has significantly advanced our understanding of cutting parameters (e.g., cutting speed, feed rate) in hard milling. Key studies have highlighted trade-offs between productivity, surface quality, and thermal effects, providing actionable strategies for industrial precision machining.

A study [21] analyzed the impact of cutting speed during hard milling using a ball-nose end-mill, evaluating surface roughness, microhardness, residual stress, and fatigue performance. Results show that surface roughness (Ra) first decreases and then increases as spindle speed rises from low to medium levels. Wu and Yin [23] employed a multi-objective genetic algorithm to optimize cutting speed and feed rate during dry milling of Cr12MoV steel, both ball-end and flat milling, and feed rate and spindle speed were identified as the primary influencing factors on surface roughness. In contrast, axial depth of cut and radial depth of cut were secondary factors. Results showed that both higher spindle speeds and lower feed rates led to reduced surface roughness. Patel and Bhavsar [24] correlated cutting parameters with forces and surface roughness during AlCrN-coated milling of D2 steel. Their experimental analysis demonstrated that while both axial depth of cut and feed rate significantly influenced cutting forces, axial depth of cut exhibited the strongest correlation with surface roughness variations. Increasing cutting speed improved surface roughness; however, increasing feed rate, axial depth of cut, or radial depth of cut increased surface roughness. During high-speed hard milling of AISI D2 steel with AlTiN-coated tools, Hazza et al. [25] identified cutting speed as the dominant factor affecting flank wear progression (contributing 70% to variance), with feed rate showing secondary influence. The authors observed that increasing cutting speed increased cutting tool wear.

Although existing research has thoroughly investigated process parameters in hard milling of steel alloys, comprehensive tool wear evaluation remains notably underexplored. Addressing this critical gap is essential, given the direct correlation between tool life and both machining efficiency and part quality. Future studies should integrate multi-objective optimization considering simultaneous wear progression and surface integrity metrics.

Recent research on AISI D2, D3, and D6 steels emphasizes machining stability in optimizing efficiency, productivity, and part quality, guiding strategies for precision and throughput in industrial applications.

Reference [26] presents a critical investigation of stability effects in high-speed milling of AISI D6 steel, demonstrating that process stabilization increases chip removal volumes, extends tool life, and improves surface finish, establishing stability as a key enabler for

sustainable high-productivity machining. In a study presented at the MATEC Web of Conferences [27], researchers systematically investigated the effects of feed rate, cutting speed, and cutter geometry on the milling of AISI D2 steel. Key findings revealed that cutting forces exhibited a strong dependence on the end-mill corner radius. Increasing cutting speed reduced cutting forces, while progressive feed rate increases elevated cutting forces. Faizu et al. [28] conducted a systematic investigation of low-speed (50–95 m/min), low-feed hard machining of AISI D2 steel (62 HRC) using TiAlN-coated carbide tools. Their comprehensive analysis revealed that surface roughness parameters (Ra and Rmax) remained remarkably stable throughout the progression of flank wear. This finding, consistent across multiple cutting parameter combinations, fundamentally challenges conventional assumptions about wear–roughness correlations in hard turning applications, suggesting that surface integrity may be preserved even during advanced tool wear stages under optimized low-energy machining conditions. Parameter optimization in trochoidal step-milling of AISI D3 steel [29] identified feed rate and step width as dominant factors affecting surface roughness under low-speed and high-feed conditions. Tool dish angle showed significant three-way interactions with cutting parameters, while microchip adhesion and lace formation were key surface degradation mechanisms. This study [30] explored the effects of cutting parameters on surface roughness and workpiece hardness during dry hard milling of steel using a coated carbide tool. Increasing spindle speed at a constant feed rate reduced surface roughness. Conversely, increasing the feed rate at a constant spindle speed increased surface roughness, due to the greater volume of chips removed per unit time.

While hard milling of cold-worked tool steel remains the most prominent method, research on milling unhardened tool steel has attracted significant interest. Key studies have investigated the effects of machining parameters on surface roughness, cutting forces, and material removal rates.

Shinge and Pable [31] investigated TiO_2 nanofluid-enhanced minimal lubrication in milling AISI D3 steel with carbide tools. They found that higher nanofluid concentrations reduced cutting temperatures and improved surface roughness. Patil et al. [32] applied Response Surface Methodology (RSM) and multi-objective learning-based optimization to input parameters to minimize surface roughness and maximize material removal rate (MRR). They found that feed rate and the interaction effects of all input parameters significantly affect surface roughness, while milling conditions influence MRR more substantially than surface roughness. Patel et al. [33] employed RSM to minimize cutting force in end-milling of AISI D2 steel with AlCrN-coated tools, identifying cutting speed and radial width of cut as dominant influencing factors.

While existing studies provide valuable insights into machining dynamics, tool life assessment remains underexplored. Given its critical impact on machining economics and efficiency, future research should prioritize investigating this factor to holistically optimize surface quality and tool longevity in demanding steel-machining applications.

A review of the literature reveals extensive research on surface roughness, tool wear, cutting forces, and temperature in machining. However, a significant gap persists: the lack of multi-objective optimization studies for minimizing surface roughness and maximizing tool life during milling of cold-worked tool steels.

Motivated by this gap, our study investigates surface roughness–tool life relationships in end-milling of AISI D2 steel (critical for demanding applications) using GC1130-coated inserts. We analyze the effects of cutting speed and feed rate to minimize surface roughness and maximize tool life simultaneously.

This study aims to achieve the following:

1. Experimentally characterize the influence of machining parameters (cutting speed and feed rate) on cutting tool life and workpiece surface roughness during wet end-milling of AISI D2 steel using GC1130-coated inserts. It should be emphasized that this research includes cutting parameters extending beyond those recommended by the cutting tool manufacturer.
2. Establish empirical models relating input parameters to each output response using experimental data, verify model adequacy via ANOVA and normal probability plots of residuals, and utilize these models for response prediction.
3. Perform multi-objective optimization of cutting speed and feed rate to simultaneously minimize surface roughness and maximize tool life using the desirability function. Overall desirability will be computed under three weighting schemes:
   Equal weights for both responses;
   Priority weighting for tool life;
   Priority weighting for surface roughness.

Together with prior works on high-speed machining and tool wear monitoring [3,7], these studies underscore the importance of integrating both extended parameters testing and wear evaluation into optimization frameworks. While several studies have optimized cutting parameters for AISI D2 steel, most remain within manufacturer-recommended ranges or address surface roughness and tool life separately. In contrast, the present work extends parameter limits beyond catalog values and employs an integrated RSM–desirability function framework to simultaneously optimize tool life and surface quality under wet machining conditions. This combination provides new practical insights into balancing productivity and surface integrity.

This study advances the understanding of machining dynamics for cold-worked tool steels and provides practical guidance for optimizing industrial processes. By identifying parameters that balance workpiece surface roughness and tool life, it offers a framework for enhancing the precision and efficiency of machining.

2. Materials and Methods

2.1. Material Selection

In this study, AISI D2 cold-worked tool steel served as the primary material. We performed chemical composition analysis using optical emission spectroscopy (OES), with the results detailed in Table 1. The table presents the measured concentrations of constituent elements, establishing a baseline for investigating the material's properties and behavior under experimental conditions.

Table 1. Microstructure and chemical composition of AISI D2 steel (wt.%) [34].

C	Mn	Cr	Mo	Si	V	Fe
1.45–1.70	0.4–0.6	11–12.5	0.7–1.2	0–0.6	0.15–0.30	Balance

AISI D2 cold-worked tool steel is critical for industrial applications, particularly in manufacturing cold-forming tools, dies, inserts, extrusion dies, and mandrels. When properly hardened and tempered, it exhibits exceptional wear resistance and high temper resistance, making it ideal for demanding machining environments. Its ability to maintain structural integrity under abrasive conditions significantly extends tool life, reducing the need for replacement and enhancing production efficiency. Moreover, AISI D2 steel exhibits a balanced combination of properties, including moderate toughness and fair machinability. While its impact resistance is limited compared to some tool steels, this is offset by its exceptional resistance to softening and wear, making it particularly suitable for applications

where durability and wear resistance are paramount. The steel's machinability, while not exceptional, remains adequate when proper tooling and machining parameters are employed, allowing for precise manufacturing of complex components.

Three specimens with identical dimensions (225 × 230 × 40) mm were examined. Microstructural analysis revealed fine globular pearlite with a non-uniform carbide distribution. The average hardness, measured at multiple locations, was 260 HB. Each specimen contained six precisely machined cavities (70 × 55 × 10) mm on its working face, totaling 12 test zones per sample. This standardized cavity geometry ensured consistent testing conditions across all specimens.

The end-milling operation was performed on a 5-axis CNC vertical machining center (Kondia HM-1000, Elgoibar, Spain) with the following specifications: maximum spindle speed of 15,000 rpm. The experiment setup is shown in Figure 1.

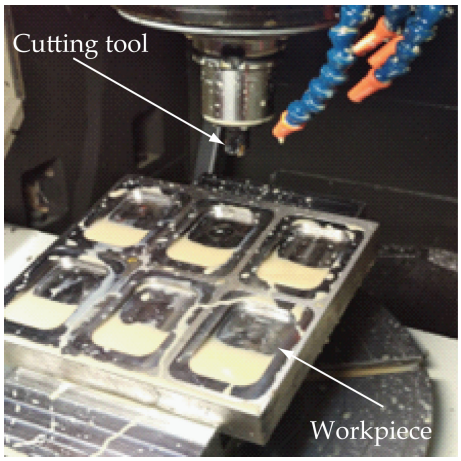

Figure 1. Experimental setup.

2.2. Cutting Tool Selection

A 25 mm diameter face mill with a cylindrical shank and three cutting inserts was employed. The inserts (Sandvik CoroMill® R390-11 T3 08M-PM, grade GC1130, Sandviken, Sweden) featured PVD ALTICRN coating and were mounted in a Sandvik R390-025B25-11M cutter body (Sandviken, Sweden).

The GC1130 grade is specifically engineered for general-purpose milling of stainless steels and high-temperature alloys, providing a balance between toughness and wear resistance. It is particularly optimized for steel machining under diverse conditions and is recommended as the primary choice for shoulder milling within the ISO P material group. The Sandvik CoroMill R390-025B25-11M is a small-diameter, high-precision, shank-type milling cutter designed for creating accurate square shoulders, faces, and slots on smaller workpieces. Its pin-lock design and use of positive rake inserts make it a capable tool for achieving excellent surface finishes and dimensional accuracy.

2.3. Experimentation and Cutting Process Parameters

The experiment was meticulously conducted using a full-factorial design with two independent variables and four levels each, with two replicates, resulting in thirty-two individual test runs. A full-factorial design provides complete coverage of the factor space, which is suitable for building regression models (e.g., quadratic models) for each response. Within this design, two critical input factors were systematically varied: the feed rate (f) in millimeters per tooth (mm/t) and the cutting speed (v) in meters per minute (m/min), both of which played pivotal roles in shaping the machining process. The levels for cutting speed and feed rate were selected based on manufacturer recommendations but extended

beyond the typical range (265–280 m/min cutting speed; 0.08–0.2 mm/t feed rate) to test the working limits of the tool–workpiece combination. Specifically, the lowest and highest levels were chosen to evaluate performance boundaries. Exploring cutting parameters beyond the manufacturer's recommended cutting speeds and feed rates represents a high-risk, high-reward strategy. Such investigations are typically undertaken by experienced machinists and process engineers who are capable of closely monitoring operations and assessing the resulting effects. This consideration raises a pertinent research question: why not systematically evaluate emerging cutting tool materials across a broader spectrum of cutting parameters to optimize both performance and tool life?

Manufacturer catalog cutting data are generally conservative, providing baselines that account for variability in machines, workpiece conditions, and operator skills. Deviations from these values—either higher or lower—may enhance productivity or quality, provided that process stability, thermal effects, and tool wear remain within acceptable limits for the specific tool–workpiece–machine system.

Excessive machining parameters can result in tool breakage or accelerated wear. A high feed per tooth degrades surface finish, while excessive combinations of feed, depth of cut, and width of cut induce chatter marks. Additionally, burr formation occurs when feed and depth of cut are too high [35].

An excessive cutting speed generates heat, accelerating tool wear, reducing hardness, and causing poor surface finish, lower material removal rates, and potential tool breakage. High temperatures can also distort the workpiece, compromising accuracy. On the other hand, an excessively low cutting speed reduces material removal rates, extending machining time. It can also cause poor chip formation, increase tool–workpiece friction, accelerate tool wear, and degrade surface finish due to inconsistent cutting [36].

Also, feed rate plays a crucial role in determining machining efficiency and part quality. If the feed rate is too high, it can lead to excessive tool wear, rough surface finish, and potential tool breakage. Conversely, a low feed rate may result in slower material removal and longer machining times, impacting productivity. Striking the right balance in feed rates is necessary to maintain part accuracy, ensure optimal material removal rates, and prolong tool life [36].

The selected levels are detailed in Table 2 for reference. A water-based emulsion cutting fluid was used with a flow rate of 8 L/min, ensuring stable wet machining conditions throughout the experiments. Two key dependent variables were accurately tracked and measured throughout the experiment: lateral surface roughness and the cutting tool life. These parameters served as critical indicators of the machining performance and quality of the processes under investigation. To ensure the robustness and reliability of our findings, each combination of input factors and levels was tested twice, yielding two replicates for every experimental condition. This duplication of tests bolstered the statistical significance of our results and enhanced the overall confidence in the conclusions drawn from the experimentation.

Table 2. Details of items required for milling tests.

Items	Details
Machine tool	HM-1000 Vertical Machining Center
Work sample	AISI D2 steel
Cutting tool	GC1130 with ALTICRN PVD coating, Sandvik
Cutting speed (v), m/min	220, 250, 280, 310
Feed per tooth (f), mm/t	0.06, 0.08, 0.2, 0.25
Depth of cut (a), mm	0.15
Cutting environment	Cutting fluid

The establishment of the tool life endpoint was guided by the ISO 8688-1:1989 [37] standard, which stipulates flank wear (VB) as the principal failure criterion due to its significant influence on tool geometry and, consequently, workpiece dimensional accuracy. The maximum acceptable flank wear was set at 0.3 mm. This value falls within the standard's typical range of 0.3–0.5 mm and was selected to reflect the requirements of a finishing process, where controlling part dimensions is critical, unlike roughing operations, which permit a higher wear limit of 0.5 mm.

The measurement of cutting tool life and surface roughness was carried out in the same cutting time range. When the flank wear reached 0.3 mm, the tool life and surface roughness were recorded. To select the machining time, some milling tests before the experiment were performed and were carried out according to the literature [12,19,26,38,39].

The machining operation itself was meticulously monitored and controlled, with the primary objective of maintaining optimal cutting tool performance. This involved a proactive approach of periodically pausing the machining process at specific time intervals. These intervals were strategically determined, taking into consideration the tool wear rates and the prevailing cutting conditions. Notably, when the cutting parameters were set to higher levels, indicating more demanding machining conditions, the chosen intervals for inspection became progressively shorter. This approach enabled real-time adjustments and immediate responses to changing tool wear rates, thereby enhancing both efficiency and tool life. It is important to highlight that the selection process for the order of testing samples, inserts, and experimental runs was deliberately randomized. This randomization minimized the potential for bias and ensured that the experimental results would be robust and statistically significant. This careful approach to the experimental design was essential for achieving reliable and reproducible outcomes in the study. For a detailed visual representation of the research methodology, please consult Figure 2.

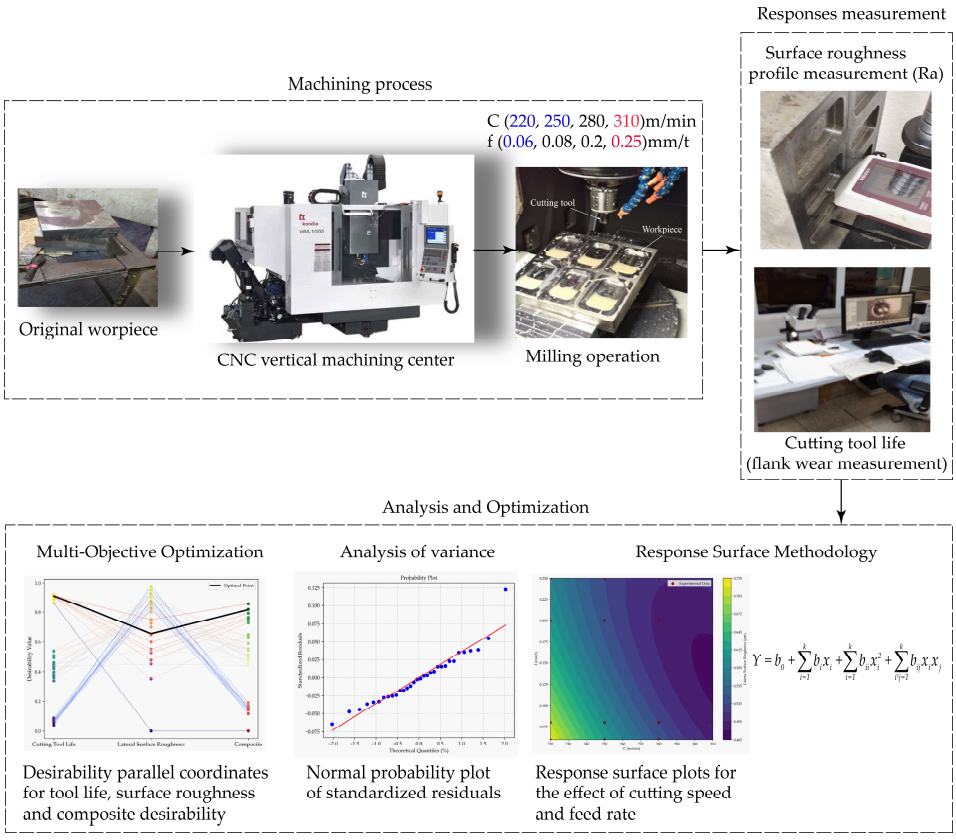

Figure 2. Research methodology.

2.4. Response Variable

To assess the surface roughness of the machined workpieces, we employed a Mitutoyo SJ-210 Roughness Tester (Kawasaki, Kanagawa, Japan). The wear and condition of the flank surfaces were meticulously examined and quantified using a Leica EY4 optical microscope (Wetzlar, Germany). Furthermore, to ensure precise and accurate positioning of the cutting tool, we relied on the precision of a Tool Master Octa pre-setting machine (Steg, Valais, Switzerland). In addition to these measurements, the hardness of the test samples was determined with utmost precision using a Brinell Nexus 3000 hardness tester (Maastricht, The Netherlands). Five indentations were performed for each condition. The applied load was specified as per the Brinell testing standards, with a holding time of 10 s. This comprehensive array of measurement and inspection tools enabled us to evaluate the quality and performance of our machining processes thoroughly.

2.5. Multi-Objective Optimization Using the Desirability Function Approach

2.5.1. Definition of Objectives

The optimization problem involves multiple response variables (Y_1, Y_2, …, Y_n), each with a defined goal: to be maximized, minimized, or targeted to a specific value. The objective of the study is to determine the optimal factor settings (X_1, X_2, …, X_k) that yield desirable outcomes for all responses.

Predictive models are developed for each response variable using Response Surface Methodology (RSM). As a widely adopted design of experiments (DOE) approach, RSM systematically evaluates the influence of input variables on output responses, including applications in machining parameter optimization. This method enables the identification of an optimal set of input variables with fewer trials, reduced effort, and minimal time compared to traditional experimental approaches. Response Surface Methodology is an empirical modeling approach that combines mathematical and statistical techniques, particularly regression analysis, to optimize an output response (dependent variable) influenced by multiple input parameters (independent variables). These models describe each response as a function of the process variables. The generalized relationship can be expressed as:

$$Y = f(x_1, x_2) \tag{1}$$

The generalized quadratic model for the output response is as follows:

$$Y = b_0 + \sum_{i=1}^{k} b_i x_i + \sum_{i=1}^{k} b_{ii} x_i^2 + \sum_{i=1}^{k} b_{ij} x_i x_j \tag{2}$$

where:

x_i, x_j: independent input variables (cutting speed and feed rate).

Y: tool life (T) and lateral surface roughness (S) as output responses.

2.5.2. Analytical Approach

The methodology employed analysis of variance (ANOVA) to evaluate the statistical significance of independent variables on both surface roughness (Ra of lateral surfaces) and cutting tool life. Model adequacy was rigorously verified through residual analysis, which examined the differences between experimentally measured values (surface roughness and tool life) and model-predicted values. All data analyses and statistical modeling were carried out using the Minitab 19 software.

2.5.3. Construction of Individual Desirability Functions

Each response is transformed into a unitless desirability scale ranging from 0 (completely undesirable) to 1 (fully desirable). The shape and bounds of each desirability function depend on the nature of the response (i.e., maximization, minimization, or targeting).

While traditional Response Surface Methodology (RSM) focuses on optimizing a single output, real-world process optimization often involves multiple—sometimes conflicting—responses. This is referred to as a multi-response optimization (MRO) problem.

In this study, the key objectives—minimizing lateral surface roughness (Ra) and maximizing cutting tool life—exhibit an inherent conflict, necessitating the use of MRO techniques. To address such challenges, various methods have been developed, including the desirability function approach (DFA) and loss function approach [40].

Among MRO techniques, the desirability function approach (DFA) stands out for its simplicity and practicality, making it highly accessible for industry practitioners. DFA transforms multi-objective problems into a single-objective framework through mathematical conversions.

$$X_{ik} = (x_{i1}, x_{i2}) = (T_{i2}, S_{i2}) \tag{3}$$

where:

Xi = input variable value for i in the experiment, i = 1, 2,. . ., m.

S fitted response model is developed for all outputs with the regression equation:

$$\hat{Y}_{ij}(x_i) = b_{j0} + \sum_{k=1}^{p} b_{jk} x_{ik} + \sum_{k=1}^{p} b_{ikk} x_{ik}^2 + \sum_{k=1}^{p} b_{ikl} x_{ik} x_{il} \tag{4}$$

$$k = 1, 2, \ldots, p$$

In case I, the smaller the better:

$$d_{ij}(\hat{Y}_{ij}) = \begin{cases} 1 & if \cdot \hat{Y}_{ij}(x_i) < G_{ij} \\ \left(\frac{\hat{Y}_{ij}(x_i) - N_{ij}}{G_{ij} - N_{ij}}\right)^{s} & if \cdot G_{ij} \le \hat{Y}_{ij}(x_i) \le N_{ij} \\ 0 & if \cdot \hat{Y}_{ij}(x_i) > N_{ij} \end{cases} \tag{5}$$

In case I, the larger the better:

$$d_{ij}(\hat{Y}_{ij}) = \begin{cases} 0 & if \cdot \hat{Y}_{ij}(x_i) < M_{ij} \\ \left(\frac{\hat{Y}_{ij}(x_i) - M_{ij}}{G_{ij} - M_{ij}}\right)^{t} & if \cdot M_{ij} \le \hat{Y}_{ij}(x_i) \le G_{ij} \\ 1 & if \cdot \hat{Y}_{ij}(x_i) > G_{ij} \end{cases} \tag{6}$$

where s and t are defined as the form of the function or weight.

2.5.4. Assignment of Importance Weights

Each response variable is assigned a weight to indicate its relative importance in the optimization process. These weights serve two key purposes: (1) enabling prioritization among competing responses, and (2) directly influencing the composite desirability index calculation.

2.5.5. Calculation of the Overall Desirability Index (D)

The composite desirability index (D) is computed by aggregating individual desirability values through a weighted geometric mean. The general formulation is expressed as:

$$D_i = \left[d_{i1}(\widehat{Y}_{i1}) \times d_{i2}(\widehat{Y}_{i2}) \times \ldots \times d_{in}(\widehat{Y}_{in}) \right]^{1/n} \tag{7}$$

where d_i is the desirability of the i-th response, and $0 \leq D_i \leq 1$.

2.5.6. Optimization Process

The optimal factor combination that maximizes Di is determined through either numerical optimization algorithms or an exhaustive grid search, selected based on the model's complexity and the characteristics of its response surface.

2.5.7. Validation of the Optimal Solution

The optimal solution is validated through both computational prediction of responses at optimal settings and, when practicable, experimental confirmation.

2.5.8. Presentation of Results

The Results section systematically presents the optimization methodology, mathematical models, identified optimal parameters, and predicted response values. Both individual and overall desirability indices are reported, supported by response surface plots and desirability function visualizations that enhance the interpretation of the multi-objective optimization outcomes.

3. Results and Discussion

This work investigates multi-response optimization in wet AISI D2 steel end-milling, aiming to maximize a composite desirability function that simultaneously addresses tool life (maximization) and surface roughness (minimization) by adjusting cutting speed and feed rate.

3.1. Definition of Objectives

The optimization problem involves multiple response variables (T and S), each with a defined goal: to be maximized (cutting tool life) and minimized (lateral surface roughness). The objective of the study is to determine the optimal factor settings (cutting speed and feed rate) that yield desirable outcomes for all responses. For clarity, the experimentally measured surface roughness and tool life values under each cutting condition are summarized in Table 3. These data serve as the basis for subsequent regression modeling and optimization.

Table 3. Experimentally measured surface roughness and tool life under different cutting conditions.

Cutting Speed (m/min)	Feed Rate (mm/tooth)	Surface Roughness Ra (μm)	Tool Life (min)
220	0.06	0.522	11.10
220	0.08	0.546	10.80
220	0.20	0.690	9.00
220	0.25	0.587	11.03
250	0.06	0.567	10.20
250	0.08	0.591	9.90
250	0.20	0.735	8.50
250	0.25	0.640	9.60
280	0.06	0.612	8.40
280	0.08	0.636	8.10
280	0.20	0.780	6.70
280	0.25	0.685	7.60
310	0.06	0.657	6.20
310	0.08	0.681	5.90
310	0.20	0.825	4.50
310	0.25	0.730	5.20

3.2. Predictive Models Are Constructed for Each Response Variable Using Response Surface Methodology

3.2.1. Model Development for Surface Roughness

The Response Surface Methodology (RSM)-derived predictive equation for lateral surface roughness (S) as a function of cutting parameters is presented below. The second-order polynomial model (Equation (8)) quantitatively relates surface roughness to cutting speed (v), feed rate (f), and their interactive effects (C × f).

$$S = 2.779 - 0.01309 \times v - 3.418 \times f + 1.875 \times 10^{-5} \times v^2 + 0.0089 \times v \times f + 2.323 \times f^2 \quad (8)$$

The R^2 statistic evaluates our model's explanatory power, specifically indicating (1) what percentage of the S variability the model accounts for, and (2) how effectively it represents the true process behavior.

The R^2 value of 81.09% demonstrates that over four-fifths of the S variability is explained by cutting speed, feed rate, their interactions, and the model structure. This indicates excellent capture of surface roughness patterns.

Robustness verification: The adjusted R^2 (77.45%) value confirms the reliability despite model complexity. An only 3.64% drop from R^2 suggests minimal overfitting. The model maintains > 75% explanatory power after penalizing it for additional variables.

Practical implications: The model validity is statistically confirmed for process optimization, surface roughness prediction, and parameter effect analysis.

The study first conducted ANOVA to statistically assess how machining parameters affect lateral surface roughness (S). The results (Tables 4 and 5) quantify each factor's influence, establishing which variables most significantly impact surface roughness.

Table 4. Analysis of variance for the response surface quadratic model of surface roughness.

Source	Degrees of Freedom	Sum of Squares	Mean Square	f	*p*
Regression	5	0.17587	0.03517	22.30	0.000
Error	26	0.04101	0.001577		
Total	31				

Table 5. Analysis of variance for second-order response surface model of surface roughness.

Source	Coefficient Estimate	Standard Error	T	*p*
Intercept	2.77945	0.553281	5.02357	0.000
f	−3.41849	1.02429	−3.33744	0.0026
C	−0.01309	0.0041581	−3.14876	0.0041
f×C	0.00890	0.0026231	3.39573	0.0022
f^2	2.32264	2.453	0.94685	0.3524
C^2	0.00001	0.000007	2.40338	0.0237

In statistical hypothesis testing, the *p*-value measures the evidence against the null hypothesis (H_0), which states that the studied factors have no real effect. If the *p*-value falls below a predetermined significance level ($\alpha = 0.05$), it provides strong evidence to reject H_0.

The model exhibited statistical significance at a 95% confidence level ($p < 0.05$; Table 3). ANOVA results ($\alpha = 0.05$) revealed that cutting speed (v), feed rate (f), and their interaction (C × f) significantly influenced surface roughness (S) (all $p < 0.05$), whereas the quadratic

feed rate term (f^2, $p = 0.352$) was insignificant (Table 5). All significant terms exceeded the 95% confidence threshold when tested against the residual mean square error.

To mitigate the risk of biased predictions and enhance the model's applicability to real-world machining scenarios, we addressed the model residuals. This included evaluating normality using a normal probability plot of standardized residuals against theoretical quantiles.

Figure 3 is key to evaluating the model's residual distribution for surface roughness. The plot shows residuals closely following a straight line, visually confirming their approximate normal (bell-shaped) distribution—a critical assumption for valid statistical analysis. This alignment suggests that the residuals meet the normality assumption required for valid statistical inference, reinforcing confidence in the model's results. Furthermore, this adherence to normality supports the model's reliability in capturing the relationship between independent variables and surface roughness, as significant deviations could indicate violations of underlying assumptions (e.g., omitted variables or incorrect functional form).

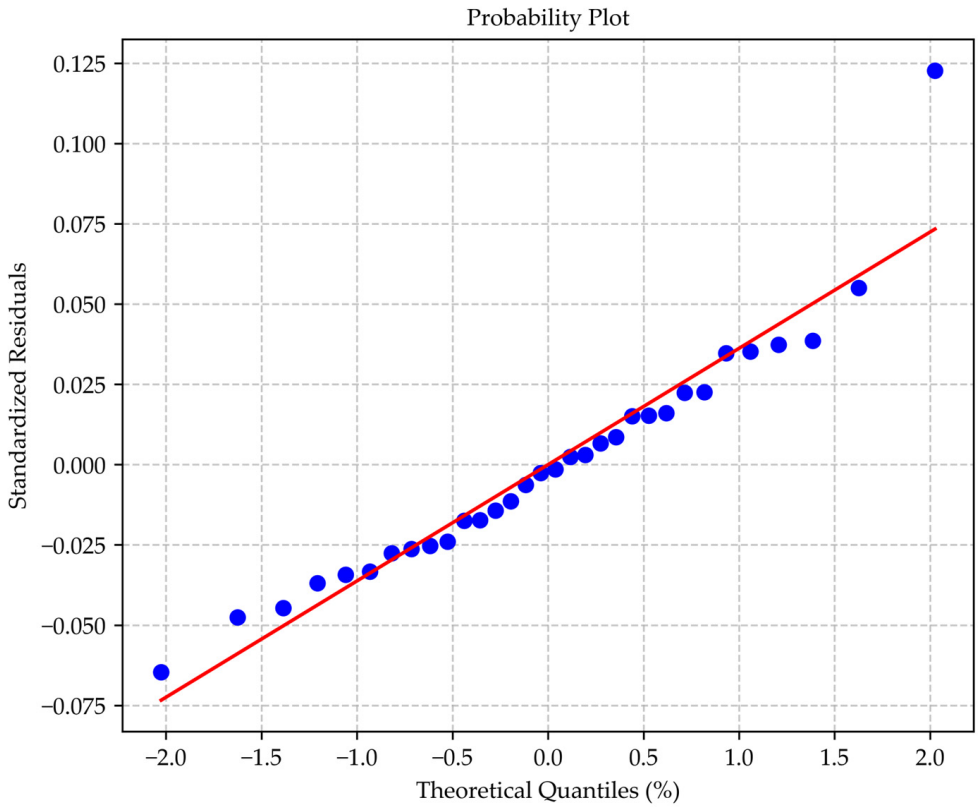

Figure 3. Normal probability plot of standardized residuals for lateral surface roughness.

The absence of systematic errors in Figure 3 further validates the model's predictive power, making it a dependable tool for decision-making.

Figure 4 demonstrates the combined effect of cutting speed and feed rate on surface roughness (Ra), two critical machining quality parameters. The analysis reveals a clear relationship, showing that higher cutting speeds (300–310 m/min) and medium feed rates (0.10–0.18 mm/t) produce the optimal surface finish, with Ra values ranging from 0.465 to 0.469 µm. This provides actionable guidance for process optimization to meet specific surface finish requirements.

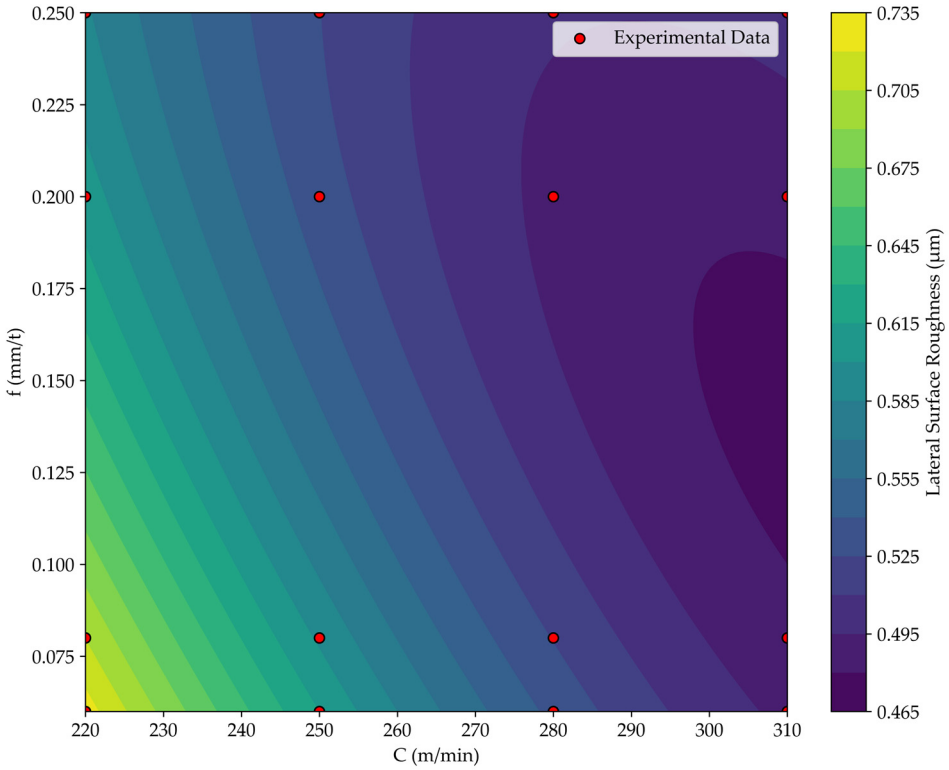

Figure 4. Response surface plots for the effect of cutting speed and feed rate on surface roughness (Ra).

The analysis indicates a general trend of decreasing surface roughness (Ra) with in-creasing cutting speeds and medium feed rates; however, the observed variation is relatively modest. Specifically, changes in cutting speed and feed rate result in an Ra variation of only 0.27 µm, suggesting that while these parameters do affect surface quality, their in-dividual impact is limited. The small range of variation implies that additional factors likely contribute to surface roughness, underscoring the need to consider a broader set of variables in machining optimization. This interpretation is further supported by the coefficients of variation: 12.85% for cutting speed, 54.97% for feed rate, and 15.02% for S.

The inverse relationship between cutting speed and surface roughness observed in our study is consistent with established findings in the machining literature [14,15,23,24,41,42]. This alignment with prior research reinforces the validity of our results while confirming a well-documented phenomenon in material removal processes. It is well established in machining theory that increasing cutting speed typically improves surface roughness. This phenomenon can be attributed to thermal softening of the workpiece material, which occurs due to elevated temperatures at higher cutting speeds. The reduced material strength at these temperatures facilitates smoother material removal, thereby enhancing surface finish [14].

However, contrasting results were reported by Vila et al. [16], who observed increased surface roughness when machining AISI D3 hardened steel using PVD AlCrN-coated carbide inserts under compressed-air cooling at low cutting speeds (60–100 m/min). These discrepancies may stem from variations in (1) cutting tool characteristics (geometry, material, coating, tooth count), (2) cutting conditions (lubrication, specific parameter combinations), and others.

On the other hand [43], during milling of AISI H13 steel with different geometrical inserts and in machining of AISI 321 stainless steel [44], these studies reported an initial worsening of surface roughness with increasing cutting speed, followed by an improvement beyond a certain threshold. Meanwhile, in high-speed face milling of AISI H13 hardened

steel using coated carbide tools, Cui and Zhao [45] reported a modest increase in surface roughness between 500 and 1500 m/min and a substantial increase up to 3000 m/min. Separately, Abbas et al. [46] observed a notable rise in surface roughness over the cutting speed range of 60–120 m/min during dry end-milling of Stainless Steel 316 with solid tungsten carbide inserts.

Similarly, the influence of feed rate on surface roughness, as observed in our study, does align with the prevailing consensus in all cases. While some sources [42,44] indicate that increasing the feed rate leads to a decrease in Ra, our results contradict this trend. In contrast to these findings, the majority of the literature sources [14,16,20,24,43,46] suggest that increasing the feed rate typically increases surface roughness. This divergence in findings highlights the complexity of machining processes and underscores the importance of considering specific cutting conditions and materials when analyzing the effect of feed rate on surface finish.

The surface roughness values obtained in this study are notably favorable, corresponding to the "very good" category. The measured Ra ranged from 0.465 to 0.735 µm, whereas typical average surface roughness for comparable operations usually lies between 0.63 and 0.8 µm [47]. Reports in the literature [48,49] similarly confirm that high-speed milling can deliver sub-micron roughness values comparable to ground surfaces. Thus, while grinding remains indispensable for ultra-fine finishing, optimized milling offers a cost-effective alternative.

3.2.2. Cutting Tool Life

The estimated equation for cutting tool life by RSM under different parameters (cutting speed and feed rate) is shown (9).

$$T = 49.71 - 0.2437 \times v + 3.815 \times f + 0.0002924 \times v^2 - 0.01254 \times v \times f + 8.462 \times f^2 \quad (9)$$

The R^2 statistics reveal that this modified model effectively accounts for 95.02% of the variance in T. Furthermore, the adjusted R^2 statistic stands at an impressive 94.06%. These metrics underscore the high quality of the obtained model.

ANOVA (Tables 6 and 7) formed a critical component of our analytical approach, enabling rigorous evaluation of factors affecting cutting tool durability. We specifically examined the effects of cutting model, speed, feed rate, and their interactions on tool life.

Table 6. Analysis of variance for the response surface quadratic model of cutting tool life.

Source	Degrees of Freedom	Sum of Squares	Mean Square	f	*p*
Regression	5	299.852	59.9704	99.18	0.000
Error	26	15.7205	0.60463		
Total	31	315.573			

Table 7. Analysis of variance for second-order response surface model of the cutting tool life.

Source	Coefficient Estimate	Standard Error	T	*p*
Intercept	49.7065	10.8317	4.589	0.0001
f	3.8146	20.0526	0.190229	0.850
C	−0.24372	0.081404	−2.994	0.006
f×C	−0.012545	0.051353	−0.24428	0.808
f^2	8.4617	48.0228	0.176202	0.8615
C^2	0.000292	0.000152	1.91421	0.0667

Tables 6 and 7 present statistically significant results: the model, intercept, and factor C all show p-values below 0.05. These findings confirm the meaningful influence of these terms on cutting tool life, warranting further discussion of their implications.

Figure 5 shows the normal probability plot for cutting tool life residuals. The close alignment of residuals with the straight line indicates normally distributed errors, validating the model's assumption of normality.

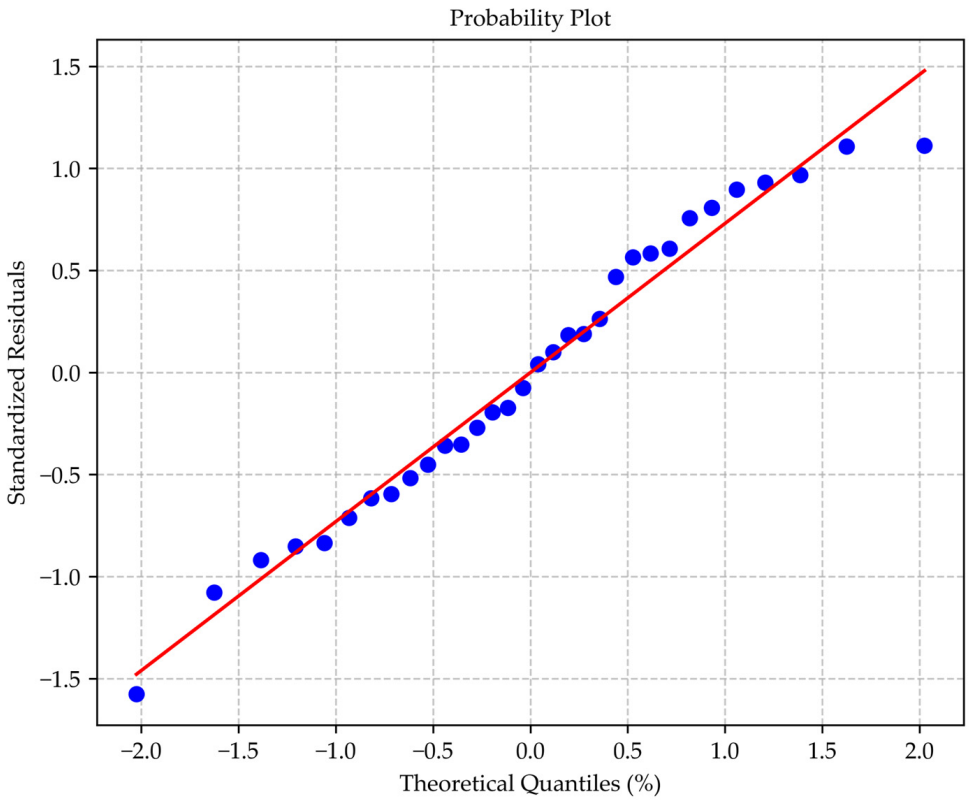

Figure 5. The probability of residuals plot for cutting tool life.

Figure 6 illustrates the relationship between cutting parameters and tool life (T). Key observations include the following:

- The highest tool life (T ≈ 11 min) occurs at lower cutting speeds combined with higher feed rates.
- Increasing cutting speed reduces tool life.
- Feed rate demonstrates minimal influence (p = 0.850) compared to cutting speed (p = 0.006), see Table 6.
- Optimal performance (T > 10 min) is achieved within a cutting speed range of 220–230 m/min, independent of feed rate.

The inverse relationship between cutting speed and tool life—where higher speeds accelerate tool wear—aligns with Taylor's model and prevailing machining studies [10,15,25,28,50]. However, it is noteworthy that tool life exhibits virtually no change as feed rate increases, contrary to conventional expectations, as indicated by references [9,28].

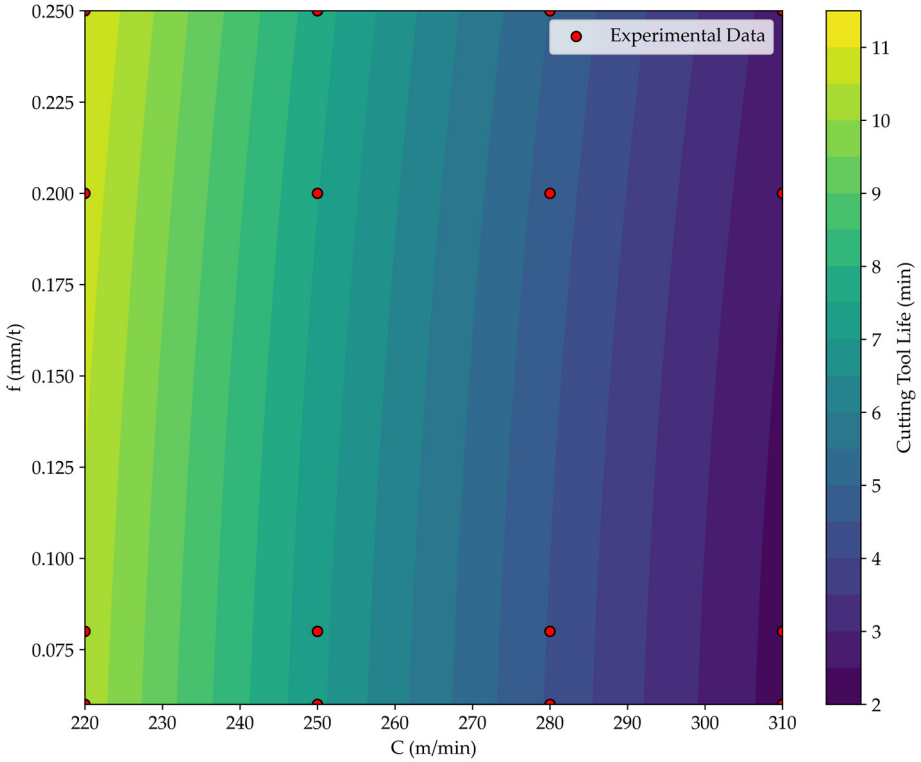

Figure 6. Response surface plots for the effect of cutting speed and feed rate on cutting tool life.

4. Construction of Individual Desirability Functions

Experimental targets for inputs (cutting speed, feed rate) and outputs (tool life, surface roughness) were based on the optimization criteria outlined in Table 8. Input values were bound by experimental ranges, with optimization limits informed by RSM contour analysis and optimal parameters sourced from the literature.

Table 8. Optimization criteria for input parameters.

Variable	Variables	Target	Lower Bound	Upper Bound
Independent	Cutting speed (m/min)	In range	220	310
	Feed rate (mm/t)	In range	0.06	0.25
Dependent (response)	Surface roughness (μm)	Minimize	0.46	0.85
	Tool life (min)	Maximize	1.92	11.13

Individual desirability functions were assigned as follows: Equation (5) for lateral surface roughness (minimization) and Equation (6) for cutting tool life (maximization).

The individual desirability values were calculated for each experimental run. The overall desirability was computed as the geometric mean of these individual values when equal weights (w_T:w_S = 1:1) were applied. For cases with differential weighting, two specific weight distributions were considered (assigned to cutting tool life and surface roughness, respectively):

Case 2: w_T:w_S = 2:1 (tool life–surface roughness).

Case 3: w_T:w_S = 1:2 (tool life–surface roughness).

These weighted overall desirability values were calculated using Equation (7), as shown in Table 9.

Table 9. Optimum cutting parameters and corresponding responses for different weight.

Weights	Cutting Speed (m/min)	Feed Rate (mm/t)	Surface Roughness (μm)	Cutting Tool Life (min)	Overall Desirability
w_T:w_S = 1:1	220	0.25	0.587	11.03	0.8168
w_T:w_S = 2:1	220	0.25	0.587	11.03	0.8706
w_T:w_S = 1:2	232.94	0.25	0.556	9.55	0.7775

Table 9 shows that the highest overall desirability value (0.8706) corresponds to Case 2 (w_T:w_S = 2:1). This solution achieved the following:

- Maximum cutting tool life (11.03 min).
- Excellent surface roughness (0.587 μm)—only 5.6% higher than the optimal 0.556 μm.
- The lowest cutting speeds.
- The highest feed rates.

This weighting prioritizes tool life extension, aligning with production objectives to minimize machining downtime and tooling costs. Notably, surface roughness also remained near optimal due to the interdependence between cutting tool life and surface quality: higher tool life (indicating lower tool wear) consistently produces better surface finishes [1,51,52].

Assigning equal weights to all objectives yielded a composite desirability score of D = 0.8168, a 6.18% reduction compared to the tool-prioritized configuration (D = 0.8706). This suggests that targeted optimization (e.g., for tool life) outperforms balanced multi-objective approaches in this system.

Prioritizing surface roughness over cutting tool performance resulted in a 10.69% reduction in the composite desirability score (from D = 0.8706 to D = 0.7775) and a 13.42% decrease in tool life (from 11.03 min to 9.55 min). This highlights a critical trade-off: improved surface finish quality comes at the cost of reduced tool durability.

Therefore, it is recommended that Case 2 (w_T:w_S = 2:1) be the optimal solution, as it maximizes productivity while maintaining surface quality through reduced tool wear. Achieving low *Ra* values requires reduced feed rates and elevated cutting speeds; however, this combination promotes thermal loading at the cutting edge, accelerating wear mechanisms and reducing tool life. Conversely, maximizing tool life typically involves lower cutting speeds and moderate feeds, which compromise surface finish. Optimal machining parameters must therefore resolve this fundamental trade-off.

Table 10 summarizes the desirability analysis results for the weighted Case 2 (w_T:w_S = 2:1), including both individual response desirabilities (d_i) and the composite desirability (D).

Thus, Case 2 (w_T:w_S = 2:1) yields the optimal weighted compromise for milling AISI D2 steel under the studied conditions. The desirability approach offers operational flexibility, enabling users to prioritize specific responses by assigning weights (Cases 1–2).

Figure 7a illustrates the contour plot of individual desirability for surface roughness (d_S) under w_T:w_S = 2:1 weighting, depicting the effects of cutting speed and feed rate. The plot demonstrates that higher cutting speeds enhance d_S, whereas increased feed rates diminish it. Conversely, Figure 7b reveals that elevated cutting speeds markedly reduce tool life desirability (d_T) due to thermally accelerated wear. At the same time, feed rate variations exert minimal influence on d_T within the tested range. This inverse relationship—where cutting speed improves d_S but compromises d_T—exemplifies the core trade-off in machining multi-objective optimization.

Table 10. Individual (d_i) and overall (D) desirability values for weighted Case 2 (w_T:w_S = 2:1).

Individual Desirability (d_i)		Overall Desirability (D)
T	S	
0.8590	0.000	0.000
0.9010	0.475	0.7278
0.9019	0.550	0.7648
0.9114	0.750	0.8541
0.4324	0.450	0.4382
0.3886	0.700	0.4728
0.4924	0.700	0.5536
0.5362	0.725	0.5929
0.3371	0.800	0.4497
0.3590	0.900	0.4877
0.3981	0.800	0.5024
0.4210	0.925	0.5473
0.0400	0.925	0.1140
0.0686	0.875	0.1602
0.0762	0.875	0.1719
0.0705	0.850	0.1616
0.8857	0.350	0.6500
0.8990	0.525	0.7515
0.9095	0.600	0.7918
0.9171	0.650	0.8177
0.4476	0.550	0.4794
0.4590	0.750	0.5407
0.5057	0.800	0.5893
0.5381	0.875	0.6328
0.3714	0.850	0.4895
0.3876	0.850	0.5036
0.3848	0.900	0.5108
0.4381	0.825	0.5410
0.0571	0.875	0.1419
0.0571	0.825	0.1391
0.0590	0.975	0.1504
0.0857	0.950	0.1911

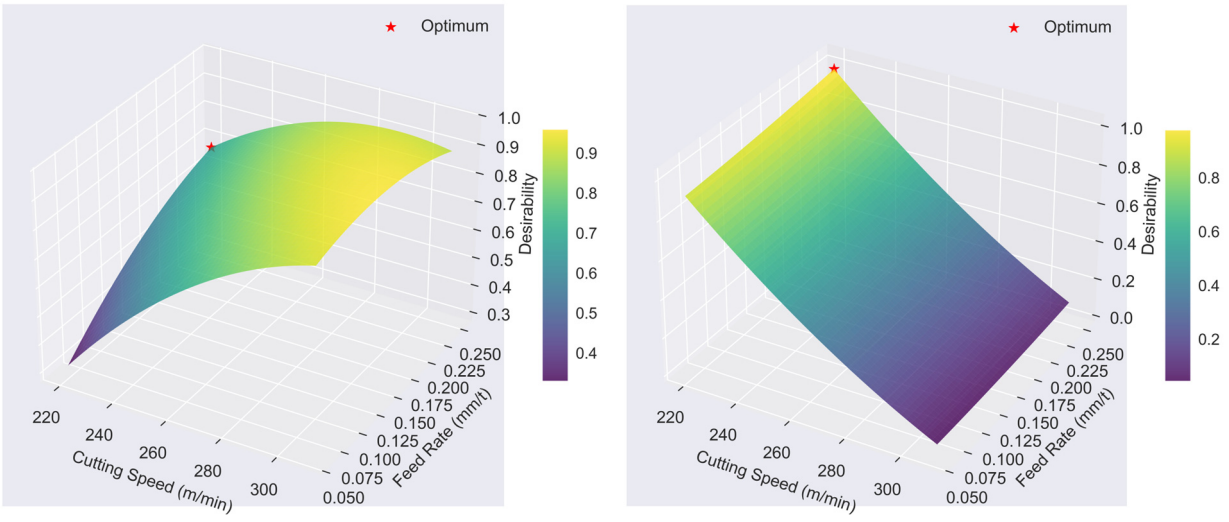

(**a**) (**b**)

Figure 7. Individual desirability graph considering the variation of cutting speed and feed rate with the w_T:w_S = 2:1 weight: (**a**) lateral surface roughness; (**b**) cutting tool life.

Figure 8a displays the 3D surface plot illustrating the effects of cutting speed and feed rate on overall desirability using a weight ratio of w_T:w_S = 2:1. The plot indicates that increasing cutting speed negatively affects overall desirability. In contrast, higher feed rates marginally increase desirability. This trend is further supported by the contour plot in Figure 8b, which corroborates the minor positive effect of feed rate on desirability.

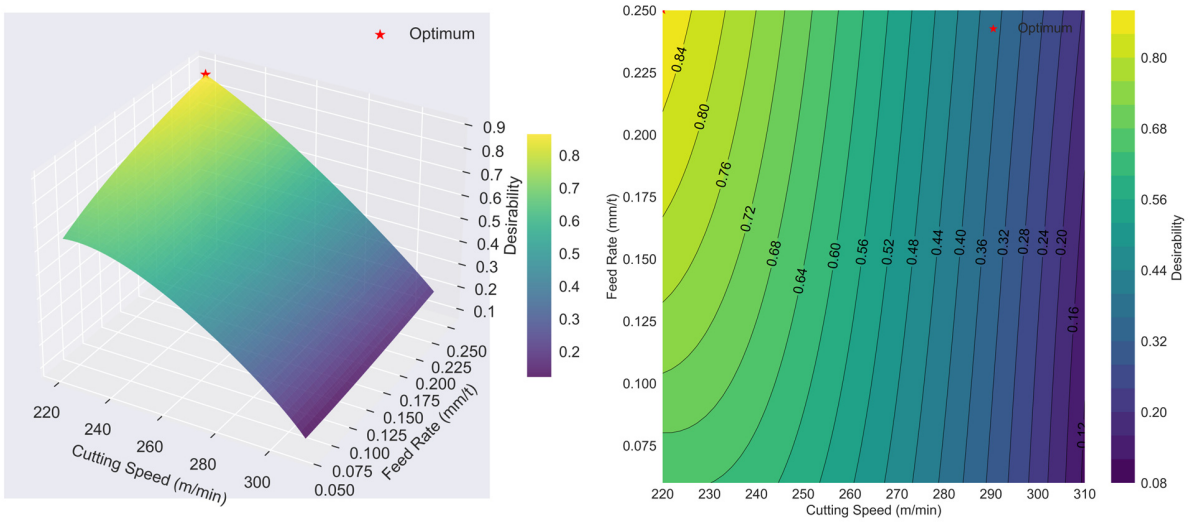

(**a**) (**b**)

Figure 8. Surface plot of the effects of cutting speed and feed rate on overall desirability with the w_T:w_S = 2:1 weight: (**a**) 3D graph; (**b**) contour plot.

This inverse relationship highlights the core machining trade-off: increased feed rate enhances productivity with a marginal improvement in composite desirability (D), whereas higher cutting speed severely compromises D through accelerated tool wear and reduced tool life.

Figure 9 illustrates a parallel coordinates plot of desirability values for tool life (d_T), surface roughness (d_S), and composite desirability (D) under a w_T:w_S = 2:1 weighting scheme. The optimal solution, representing the best compromise between conflicting objectives, is distinctly highlighted across all response axes.

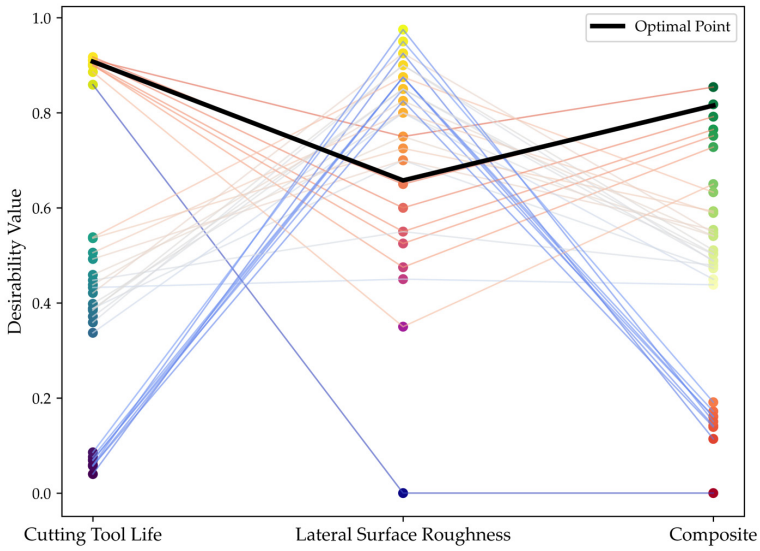

Figure 9. Parallel coordinates plot of desirability values for tool life (d_T), surface roughness (d_S), and composite desirability (D) under a w_T:w_S = 2:1 weighting scheme weight.

The desirability-based multi-objective optimization identified Pareto-optimal parameters: cutting speed = 220 m/min and feed rate = 0.25 mm/tooth. This configuration demonstrates that combining reduced cutting speeds with elevated feed rates simultaneously enhances tool life (mitigating thermal wear) and surface roughness (suppressing vibration), achieving a composite desirability of D = 0.8706 under a 2:1 weight ratio of w_T:w_S (Table 8). Notably, these parameters deviate from the manufacturer's recommendations for the cutting tool. This deviation arises because manufacturer guidelines prioritize generalized tool safety margins, whereas our optimization specifically targets enhanced productivity for steels under controlled wet machining conditions. Nevertheless, this solution provides the optimal balance between competing objectives, establishing its technical efficacy for wet milling of AISI D2 steel (260 HB) using coated GC1130 inserts.

5. Conclusions

This study presents a comprehensive experimental investigation into the effects of cutting speed and feed rate on tool life and surface roughness during wet end-milling of AISI D2 tool steel using GC1130-coated carbide inserts. The principal contribution of this work lies in the systematic evaluation of cutting parameters that extend beyond the manufacturer's recommended limits, thereby providing new insights into the potential bene-fits and limitations of operating outside conventional guidelines. This research employs an integrated optimization approach combining Response Surface Methodology (RSM) with a multi-objective framework using the desirability function approach. The methodology simultaneously addresses two competing objectives: minimizing surface roughness while maximizing tool life. The key anticipated contributions of this work include the following:

1. Response Surface Methodology (RSM) was employed to develop mathematical models that elucidate the relationships between feed rate, cutting speed, surface roughness, and tool life. The study incorporated rigorous statistical analyses, including analysis of variance (ANOVA), coefficients of determination (R^2), and residual diagnostics, to assess the adequacy and predictive accuracy of the developed models. These methodologies were essential for formulating and validating reliable mathematical representations that capture the influence of cutting parameters on surface roughness and tool life.

2. Optimal Operating Conditions. Response surface analysis revealed distinct trends in the interaction between cutting speed and feed rate. For surface roughness, optimal values were achieved at high cutting speeds with medium feed rates (both parameters being statistically significant). Conversely, maximum tool life was observed at lower cutting speeds combined with higher feed rates (although this parameter was not statistically significant). These results provide actionable guidance for industrial machining, suggesting that different parameter combinations can be selected to prioritize either surface quality or tool longevity.

3. Multi-Objective Optimization. Using a desirability function approach with three weighting scenarios (equal weights, tool-life-prioritized, and surface-roughness-prioritized), tool life prioritization was selected as the optimum solution because it highlights the highest overall desirability value (0.8706). Also, this rate achieved maximum cutting tool life (11.03 min), excellent surface roughness (0.587 μm)—only 5.6% higher than the optimal 0.556 μm—the lowest cutting speed, and the highest feed rate. This weighting prioritizes tool life extension, which aligns with production objectives to reduce machining downtime and tooling costs. Notably, surface roughness also remained near optimal due to the interdependence between cutting tool life and surface quality: higher tool life (indicating lower tool wear) consistently produces better surface roughness.

4. These results demonstrate that combining lower cutting speeds with higher feed rates significantly enhances overall machining performance, as evidenced by the high composite desirability score (D = 0.8706) for the cutting-tool-prioritized configuration. This configuration optimally balances competing objectives, outperforming the equal-weights scenario (D = 0.8168) by 6.18%. Notably, while the equal-weights scenario achieves comparable tool life and surface roughness, its lower desirability score highlights the advantage of targeted optimization for tool performance. Further, prioritizing surface roughness over cutting tool performance reduces the composite desirability score by 10.69% (from D = 0.8706 to D = 0.7775) and decreases tool life by 13.42% (from 11.03 min to 9.55 min). This underscores a critical trade-off: improved surface finish comes at the expense of tool durability. Thus, the cutting-tool-prioritized configuration emerges as the most efficient compromise for this system.

In summary, this research not only provides insight into the intricate dynamics of cutting speed and feed in end-milling operations, but it also offers practical guidance on optimizing machining conditions for improved tool life and surface quality. These findings hold great promise for enhancing the efficiency and competitiveness of machining operations.

Author Contributions: Conceptualization, L.W.H., D.A.C., and R.P.; methodology, L.W.H., Y.S.A., and R.P.; validation, L.W.H., Y.S.A., and R.P.; formal analysis, L.W.H., Y.S.A., and D.A.C.; investigation, L.W.H. and R.P.; resources, L.W.H. and R.P.; writing—original draft preparation, L.W.H., Y.S.A., and R.P.; writing—review and editing, L.W.H., Y.S.A., and R.P.; supervision, L.W.H., Y.S.A., R.P., and D.A.C.; project administration, L.W.H. and R.P. All authors have read and agreed to the published version of the manuscript.

Funding: This research received no external funding.

Data Availability Statement: The original contributions presented in this study are included in the article. Further inquiries can be directed to the corresponding authors.

Acknowledgments: The authors would like to express their sincere gratitude to Jorge Alberto Sánchez Varona for his valuable contributions to the experimental research. The authors also acknowledge the support of the Interdisciplinary Research Center for Advanced Materials (IRC-AM) at King Fahd University of Petroleum and Minerals (KFUPM) for enabling this work. The authors also acknowledge that an earlier version of this manuscript was posted as a preprint on Research Square. Although a withdrawal request has been submitted, the preprint remains accessible in the version history.

Conflicts of Interest: The authors declare no conflicts of interest.

Abbreviations

The following abbreviations are used in this manuscript:

RSM	Response surface methodology
ANOVA	Analysis of variance
R^2	Coefficients of determination
DFA	Desirability function approach
DOE	Design of experiments
MRO	Multi-response optimization

References

1. Abellán-Nebot, J.V.; Vila, C.; Siller, H.R. A review of the factors influencing surface roughness in machining and their impact on sustainability. *Sustainability* **2024**, *16*, 1917. [CrossRef]
2. De Lacalle, L.N.L.; Lamikiz, A.; Salgado, M.A.; Herranz, S.; Rivero, A. Process planning for reliable high-speed machining of moulds. *Int. J. Prod. Res.* **2002**, *40*, 2789–2809. [CrossRef]
3. de Lacalle, L.N.L.; Lamikiz, A.; Muñoa, J.; Salgado, M.A.; Sánchez, J.A. Improving the high-speed finishing of forming tools for advanced high-strength steels (AHSS). *Int. J. Adv. Manuf. Technol.* **2006**, *29*, 49–63. [CrossRef]

4. De Lacalle, L.N.L.; Lamikiz, A.; Sánchez, J.A.; De Bustos, I.F. Recording of real cutting forces along the milling of complex parts. *Mechatronics* **2006**, *16*, 21–32. [CrossRef]
5. Fernández-Abia, A.I.; Barreiro, J.; de Lacalle, L.N.L.; Martínez-Pellitero, S. Behavior of austenitic stainless steels at high-speed turning using specific force coefficients. *Int. J. Adv. Manuf. Technol.* **2012**, *62*, 505–515. [CrossRef]
6. Choudhury, I.; Elbaradie, M. Machinability assessment of inconel 718 by factorial design of experiment coupled with response surface methodology. *J. Mater. Process. Technol.* **1999**, *95*, 30–39. [CrossRef]
7. Del Olmo, A.; De Lacalle, L.N.L.; De Pissón, G.M.; Pérez-Salinas, C.; Ealo, J.A. Tool wear monitoring of high-speed broaching process with carbide tools to reduce production errors. *Mech. Syst. Signal Process.* **2022**, *172*, 109003. [CrossRef]
8. Aldekoa, I.; Del Olmo, A.; Sastoque-Pinilla, L.; Sendino-Mouliet, S.; De Lacalle, L.N.L. Early detection of tool wear in electromechanical broaching machines by monitoring main stroke servomotors. *Mech. Syst. Signal Process.* **2024**, *204*, 110773. [CrossRef]
9. Iqbal, A.; He, N.; Li, L. Empirical Modeling the Effects of Cutting Parameters in High-Speed End Milling of Hardened AISI D2 under MQL Environment. In Proceedings of the World Congress on Engineering, London, UK, 6–8 July 2011.
10. Wojciechowski, S.; Twardowski, P. Tool life and process dynamics in high speed ball end milling of hardened steel. *Procedia CIRP* **2012**, *1*, 289–294. [CrossRef]
11. Wojciechowski, S.; Twardowski, P. The influence of tool wear on the vibrations during ball end milling of hardened steel. *Procedia CIRP* **2014**, *14*, 587–592. [CrossRef]
12. Mariño, M.; Sánchez, Y. Influencia de los regímenes de lubricación en la vida de la herramienta y el acabado superficial del fresado de aceros endurecidos AISI D2 y AISI D6. *Minería Y Geol.* **2015**, *31*, 62–78.
13. Dong, P.Q.; Duc, T.M.; Tuan, N.M.; Long, T.T.; Thah, D.V.; Truong, N.V. Improvement in the Hard Milling of AISI D2 Steel under the MQCL Condition Using Emulsion-Dispersed MoS_2 Nanosheets. *Lubricants* **2020**, *8*, 62. [CrossRef]
14. Chattopadhyay, A.; Mandal, N.K.; Maity, A. An investigation on machinability of AISI D2 steel during hard milling with multi-resolution analysis of vibration. *Eng. Res. Express* **2023**, *5*, 015053. [CrossRef]
15. Ravi, S.; Gurusamy, P. Experimental investigation of cryogenic cooling on cutting force, surface roughness and tool wear in end milling of hardened AISI D3 steel using uncoated tool. *Mater. Today Proc.* **2020**, *33*, 3314–3318. [CrossRef]
16. Vila, C.; Abellán, J.V.; Siller, H.R. Study of different cutting strategies for sustainable machining of hardened steels. *Procedia Eng.* **2015**, *132*, 1120–1127. [CrossRef]
17. Saedon, J.B.; Soo, S.L.; Aspinwall, D.K.; Barnacle, A.; Mohamad, N.H. Surface integrity in micromilling of hardened AISI D2 tool steel. *Appl. Mech. Mater.* **2015**, *789–790*, 151–155. [CrossRef]
18. Gaitonde, V.; Karnik, S.; Alves, C.; Campos, J.; Mendes, A. Machinability evaluation in hard milling of AISI D2 steel. *Mater. Res.* **2016**, *19*, 360–369. [CrossRef]
19. Tlhabadira, I.; Daniyan, I.A.; Masu, L.; Van Staden, L.R. Process Design and Optimization of Surface Roughness during M200 TS Milling Process using the Taguchi Method. *Procedia CIRP* **2019**, *84*, 868–873. [CrossRef]
20. Mashood, A.; Jamil, M.; Ul, A.; Hussain, S.; Meng, L.; He, N. Sustainable machining. Modeling and optimization of temperature and surface roughness in the milling of AISI D2 steel. *Ind. Lubr. Tribol.* **2018**, *71*, 267–277. [CrossRef]
21. Huang, W.; Zhao, J.; Niu, J.; Wang, G.; Cheng, R. Comparison in surface integrity and fatigue performance for hardened steel ball-end milled with different milling speeds. *Procedia CIRP* **2018**, *71*, 267–271. [CrossRef]
22. Nguyen, Q.-M.; Do, T.-V. Optimal approaches for Hard Milling of SKD11 steel under MQL conditions using SiO_2 nanoparticles. *Adv. Mater. Sci. Eng.* **2022**, *2022*, 2627522. [CrossRef]
23. Wu, X.; Yin, X. Surface roughness analysis and parameter optimization of mold steel milling. *Procedia CIRP* **2018**, *71*, 317–321. [CrossRef]
24. Patel, R.; Bhavsar, S. Effect on surface roughness and cutting force during hard machining of AISI D2 tool steel using AlCrN coated tool using OVAT. *Int. J. Res. Anal. Rev.* **2019**, *6*, 206–211. Available online: https://ijrar.com/upload_issue/ijrar_issue_20543148.pdf (accessed on 3 September 2025).
25. Hazza, M.; Hazza, F.A.; Muhammad, K. Flank wear modelling in High Speed Hard Milling of AISI D2 steel. *Int. J. Eng. Mater. Manuf.* **2020**, *5*, 50–54. [CrossRef]
26. Sánchez, Y.; Eduardo, A.; Mariño, M. Vida y productividad de la herramienta de corte en el fresado de acabado del acero endurecido AISI D6. *Ingeniare. Rev. Chil. De Ing.* **2017**, *25*, 205–216. [CrossRef]
27. Beşliu, I.; Amarandei, D.; Cerlincă, D. Analysis of chip formation and cutting forces in end milling AISI D2 tool steel with different cutting tool geometries. In Proceedings of the MATEC Web of Conferences, Chisinau, Moldova, 31 May–2 June 2018; Volume 178. Available online: https://www.matec-conferences.org/articles/matecconf/abs/2018/37/matecconf_imanee2018_01016/matecconf_imanee2018_01016.html (accessed on 3 September 2025).

28. Faizu, N.; Awang, N.W.; Berahim, N. Tool Wear and Surface Roughness in Machining AISI D2 Tool Steel. *Indian J. Sci. Technol.* **2016**, *9*, 20–25. [CrossRef]
29. Santhakumar, J.; Iqbal, M. Parametric optimization of trochoidal step on surface roughness and dish angle in end milling of AISID3 steel using precise measurements. *Materials* **2019**, *12*, 1335. [CrossRef]
30. Ceritbinmez, F.; Kanca, E. The effects of cutting parameters used in milling X153CRMOV12 cold work tool steel by end mills on surface roughness and hardness of the workpiece. *Gazi Üniversitesi Fen Bilim. Derg. Part C Tasarım Ve Teknol.* **2022**, *10*, 27–38. [CrossRef]
31. Shinge, V.R.; Pable, M.J. Effect of nano-minimum quantity lubrication on cutting temperature and surface roughness of milling AISI D3 tool steel. *Mater. Today Proc.* **2023**, *72*, 1758–1764. [CrossRef]
32. Patil, A.; Rudrapati, R.; Poonawala, N.S. Examination and prediction of process parameters for Surface roughness and MRR in VMC-five axis machining of D3 steel by using RSM and MTLBO. *Mater. Today Proc.* **2021**, *44*, 2748–2753. [CrossRef]
33. Patel, R.D.; Bhavsar, S.N.; Patel, A.K. Experimental investigation on cutting force during end milling of AISI D2 tool steel using AlCrN coated tool. *Mater. Today Proc.* **2023**, *80*, 1397–1402. [CrossRef]
34. Mochtar, M.A.; Putra, W.N.; Abram, M. Effect of tempering temperature and subzero treatment on microstructures, retained austenite, and hardness of AISI D2 tool steel. *Mater. Res. Express* **2023**, *10*, 056511. [CrossRef]
35. Kalpakjian, S.; Schmid, S.R. Fundamentals of Machining. In *Manufacturing, Engineering & Technology*, 7th ed.; Pearson Education Ltd.: London, UK, 2014; pp. 566–599.
36. Ye, R. Feed Rate and Cutting Speed in Machining: Differences, Connection and Calculation. 2024. Available online: https://www.3erp.com/blog/feed-rate-cutting-speed-machining/ (accessed on 3 September 2025).
37. *ISO 8688-2:1989*; Tool Life Testing in Milling—Part 2: End Milling. International Organization for Standardization: Geneva, Switzerland, 1989.
38. Arsecularatne, J.A.; Zhang, L.C.; Montross, C.; Mathew, P. On machining of hardened AISI D2 steel with PCBN tools. *J. Mater. Process. Technol.* **2006**, *171*, 244–252. [CrossRef]
39. Abas, M.; Alkahtani, M.; Khalid, Q.S.; Hussain, G.; Abidi, M.H.; Buhl, J. Parametric Study and Optimization of End-Milling Operation of AISI 1522H Steel Using Definitive Screening Design and Multi-Criteria Decision-Making Approach. *Materials* **2022**, *15*, 4086. [CrossRef] [PubMed]
40. Roy, R.; Ghosh, S.K.; Kaisar, T.I.; Ahmed, T.; Hossain, S.; Aslam, M.; Kaseem, M.; Rahman, M.M. Multi-Response Optimization of Surface Grinding Process Parameters of AISI 4140 Alloy Steel Using Response Surface Methodology and Desirability Function under Dry and Wet Conditions. *Coatings* **2022**, *12*, 104. [CrossRef]
41. Chockalingam, P.; Hong, L. Surface roughness and tool wear study on milling of AISI 304 stainless steel using different cooling conditions. *Int. J. Eng. Technol.* **2012**, *2*, 1386–1391.
42. Al-Hazza, M.H.F.; bt Ibrahim, N.A.; Adesta, E.T.; Khan, A.A.; Sidek, A.B.A. Surface roughness optimization using Taguchi Method of high speed end milling for hardened steel D2. In Proceedings of the International Conference on Mechanical, Automotive and Aerospace Engineering (ICMAAE'16), Kuala Lumpur, Malaysia, 25–27 July 2016; International Islamic University Malaysia (IIUM): Kuala Lumpur, Malaysia, 2017. Available online: http://iopscience.iop.org/1757-899X/184/1/012047 (accessed on 3 September 2025).
43. Ding, T.C.; Zhang, S.; Lv, H.G.; Xu, X.L. A comparative investigation on surface roughness and residual stress during end-milling AISI H13 steel with different geometrical inserts. *Mater. Manuf. Process.* **2011**, *26*, 1085–1093. [CrossRef]
44. Holkar, H.; Sadaiah, M. Optimization of end milling machining parameters of AISI 321 stainless steel using Taguchi method. *Int. J. Recent Innov. Trends Comput. Commun.* **2016**, *4*, 20–23. Available online: http://www.ijritcc.org (accessed on 3 September 2025).
45. Cui, X.; Zhao, J.; Jia, C.; Zhou, Y. Surface roughness and chip formation in high-speed face milling AISI H13 steel. *Int. J. Adv. Manuf. Technol.* **2012**, *61*, 1–13. [CrossRef]
46. Abbas, A.T.; Anwar, S.; Abdelnasser, E.; Luqman, M.; Qudeiri, J.E.A.; Elkaseer, A. Effect of different cooling strategies on surface quality and power consumption in finishing end milling of stainless steel 316. *Materials* **2021**, *14*, 903. [CrossRef]
47. Kalpakjian, S.; Schmid, S.R. Machining Processes: Turning and Hole Making. In *Manufacturing, Engineering & Technology*, 7th ed.; Pearson Education Ltd.: London, UK, 2014; pp. 625–667.
48. Li, Z.; Dai, Y.; Guan, C.; Lai, T.; Sun, Z.; Li, H. An on-machine measurement technique with sub-micron accuracy on a low-precision grinding machine tool. *J. Manuf. Process.* **2024**, *119*, 520–530. [CrossRef]
49. Teimouri, R.; Skoczypiec, S. Predictive modeling of roughness change in multistep machining. *J. Intell. Manuf.* **2024**, *35*, 3577–3598. [CrossRef]
50. Songmene, V.; Zaghbani, I.; Kientzy, G. Machining and machinability of tool steels: Effects of lubrication and machining conditions on tool wear and tool life data. *Procedia CIRP.* **2018**, *77*, 505–508. [CrossRef]

51. Demirpolat, H.; Binali, R.; Patange, A.D.; Pardeshi, S.S.; Gnanasekaran, S. Comparison of tool wear, surface roughness, cutting forces, tool tip temperature, and chip shape during sustainable turning of bearing steel. *Materials* **2023**, *16*, 4408. [CrossRef]
52. Li, C.; Zhao, G.; Ji, D.; Zhang, G.; Liu, L.; Zeng, F.; Zhao, Z. Inflence of tool wear and workpiece diameter on surface quality and prediction of surface roughness in turning. *Metals* **2024**, *14*, 1205. [CrossRef]